Journal of Power Sources 196 (2011) 1338–1341

Contents lists available at ScienceDirect

Journal of Power Sources

journal homepage: www.elsevier.com/locate/jpowsour

Short communication

A novel bilayered $Sr_{0.6}La_{0.4}TiO_3/La_{0.8}Sr_{0.2}MnO_3$ interconnector for anode-supported tubular solid oxide fuel cell via slurry-brushing and co-sintering process

Yanjie Xu, Shaorong Wang*, Renzhu Liu, Tinglian Wen, Zhaoyin Wen

CAS Key Laboratory of Materials for Energy Conversion, Shanghai Institute of Ceramics, Chinese Academy of Sciences (SICCAS), 1295 Dingxi Road, Shanghai 200050, PR China

ARTICLE INFO

Article history:
Received 29 June 2010
Received in revised form 27 July 2010
Accepted 27 July 2010
Available online 6 August 2010

Keywords:
Tubular solid oxide fuel cell
Anode-supported
Interconnector
Slurry-brushing
Co-sintering

ABSTRACT

Considering that conventional lanthanum chromate ($LaCrO_3$) interconnector is hard to be co-sintered with green anode, we have fabricated a novel bilayered interconnector which consists of La-doped $SrTiO_3$ ($Sr_{0.6}La_{0.4}TiO_3$) and Sr-doped lanthanum manganite ($La_{0.8}Sr_{0.2}MnO_3$). $Sr_{0.6}La_{0.4}TiO_3$ is conductive and stable in reducing atmosphere, locating on the anode side; while $La_{0.8}Sr_{0.2}MnO_3$ is on the cathode side. A slurry-brushing and co-sintering method is applied: the $Sr_{0.6}La_{0.4}TiO_3$ and $La_{0.8}Sr_{0.2}MnO_3$ slurries are successively brushed onto green anode specimen, followed by co-firing course to form a dense bilayered $Sr_{0.6}La_{0.4}TiO_3/La_{0.8}Sr_{0.2}MnO_3$ interconnector. For operating with humidified hydrogen and oxygen at 900 °C, the ohmic resistances between anode and cathode/interconnector are 0.33 Ω cm^2 and 0.186 Ω cm^2, respectively. The maximum power density is 290 mW cm^{-2} for a cell with interconnector, and 420 mW cm^{-2} for a cell without it, which demonstrates that nearly 70% of the power output can be achieved using this bilayered $Sr_{0.6}La_{0.4}TiO_3/La_{0.8}Sr_{0.2}MnO_3$ interconnector.

1. Introduction

Solid oxide full cells (SOFC) represent an advanced technology for clean, high efficient and reliable energy conversion, which has attracted more and more attentions worldwide [1–3]. Tubular SOFC have many advantages such as the ease of sealing, the ability to endure the thermal stress caused by rapid heating [3–6]. However, interconnector still remains to be a main challenge holding back single fuel cells from being compiled into stacks [7,8]. Interconnector provides the conductive path for electrical current to pass from the anode of one cell to the cathode of the next one, as well as separating the fuel gas from the oxidant. So it should be completely dense, sufficiently conductive, and quite stable in both oxidizing and reducing atmospheres. Due to these tough requirements, only few materials can be adequate for SOFC interconnector. Lanthanum chromate ($LaCrO_3$) based perovskite materials are the most promising one which have high thermal and chemical stability in dual oxidation-reduction atmosphere as well as good electrical conductivity, thus have been extensively investigated [9–12]. However, their poor sintering ability makes them unable to be co-sintered with green tubular anode, resulting expensive cost for manufacturing.

This communication reports our efforts to prepare a novel bilayered $Sr_{0.6}La_{0.4}TiO_3/La_{0.8}Sr_{0.2}MnO_3$ interconnector via co-sintering with green tubular anode. La-doped $SrTiO_3$ (SLT) is studied by some researchers for SOFC anode material due to its good electrical conductivity and stabilization in reducing atmosphere [13–16]. Thus we employ it to be connected with NiO + YSZ anode. $La_{0.8}Sr_{0.2}MnO_3$ (LSM) is on the cathode side due to its high electrical conductivity and good stabilization in oxidation atmosphere. The SLT and LSM slurries were successively brushed onto green anode specimen, followed by co-firing course to form a dense bilayered SLT/LSM interconnector. Microstructure and combination between the bilayered interconnector and the anode were studied by SEM, AC impedance spectra and current–voltage (*I–V*) curves were employed to determine the properties of single cells with and without interconnector.

2. Experimental

2.1. Powder and slurry preparation

To prepare SLT powder by solid-state reaction method, stoichiometric ratio of $SrCO_3$, La_2O_3 and TiO_2 was mixed by ball-milling. After that, the mixture was dried, die-pressed, and heated at 1200 °C for 5–8 h. Then, the powder was ball-milled again for further use. LSM powder was provided by Fuel Cell Materials Corporation.

* Corresponding author. Tel.: +86 21 52411520; fax: +86 21 52411520.
E-mail address: srwang@mail.sic.ac.cn (S. Wang).

0378-7753/$ – see front matter © 2010 Elsevier B.V. All rights reserved.
doi:10.1016/j.jpowsour.2010.07.088

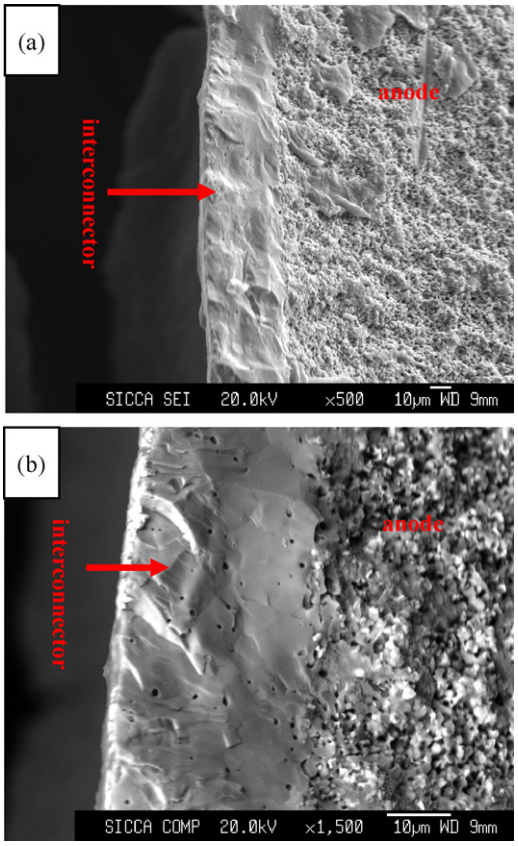

Fig. 1. Cross-section SEM micrographs of (a) co-sintered interconnector and anode, (b) enlarged (a).

To prepare the slurries for brushing, the powders of SLT and LSM were mixed with an appropriate binder system (i.e. ethanol, PVB, triethanolamine), respectively. The triethanolamine (TEA) was helpful for the powders to disperse homogeneously, with the mass percentage of 3% to the powders; while PVB was added in order to enhance the viscosity of slurries, with the mass percentage of 2% to the powders. The mass ratio of powder to ethanol was 1:2 for SLT slurry, and 1:1.5 for LSM slurry. Then the two slurries were ball-milled for about 3 h, respectively, followed by vacuum pumping for several minutes to eliminate air bubbles.

2.2. Slurry-brushing process

Firstly, green tubular anode consisting of NiO and YSZ was fabricated via dip-coating process (details can be found elsewhere [17]). Secondly, a SSZ (Sc doped ZrO_2, from Daiichi Kigenso Kagaku Kogyo, Japan) electrolyte layer was coated onto green tubular anode by dip-coating too. Thirdly, erase a rectangular area of SSZ along the axial direction by 0.6 cm × 4.5 cm, in order to brush SLT slurry onto the exposed anode area.

Then, SLT slurry was brushed onto green anode by a brush pen, until the SSZ-free area was completely covered by SLT slurry, especially the boundary of green anode and SSZ electrolyte. Otherwise, fuel gas or oxygen could penetrate through the boundary which would reduce the open circuit voltage of SOFC (OCV). The LSM slurry was brushed onto the SLT layer subsequently. Finally, the green tubular anode with SSZ electrolyte and bilayered SLT/LSM were co-fired at 1400 °C for 3–5 h.

2.3. Cathode fabrication

The LSM/SSZ composite cathode was fabricated by dip-coating method. 70 g LSM and 30 g SSZ were mixed with 60 g methyl ethyl ketone (MEK) and 50 g ethanol by ball-milling for 1–2 h, using 5 g TEA as dispersant. Then, 8 g PVB, 10 g polyethylene glycol and 10 g dibutyl-O-phthalate were added into the slurry in order to enhance the viscosity and avoid the coating cracking. The slurry was ball-milled for another 1–2 h, followed by vacuum pumping for several minutes to eliminate air bubbles. Before dip-coating, the interconnector was covered by adhesive tape, in order to separate it from LSM/SSZ cathode slurry. There was an empty area between cathode and interconnector serving for insulating. Otherwise, cathode would be connected with anode via interconnector, leading to inner short-circuit. The cathode was heated at 1200 °C for 3 h, and a single tubular SOFC with interconnector was obtained. The diameters of tubular cells were about 11.16 mm, and the length of cathode was about 40–60 mm which depended on the dip-coating method.

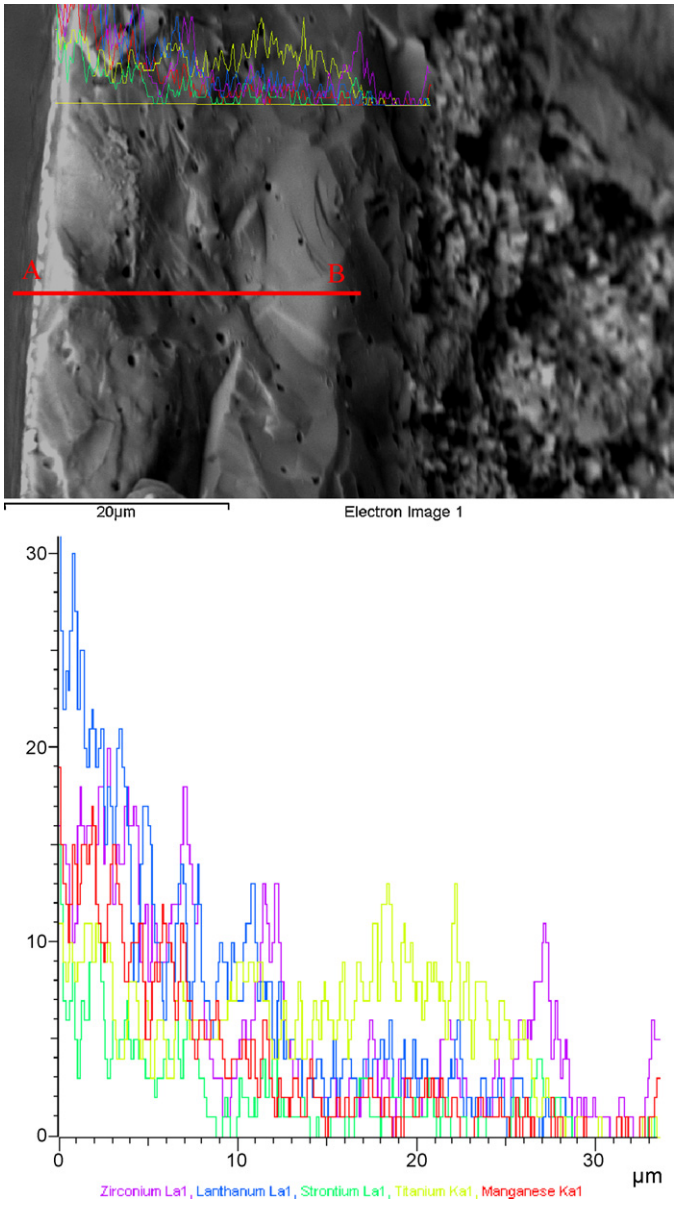

Fig. 2. EDS line-scan images through cross-section of co-sintered interconnector and anode.

2.4. Cell performance test

Tubular SOFC tests were carried out by four-probe method. There were two pt-wires fixed on anode, cathode and intercon-

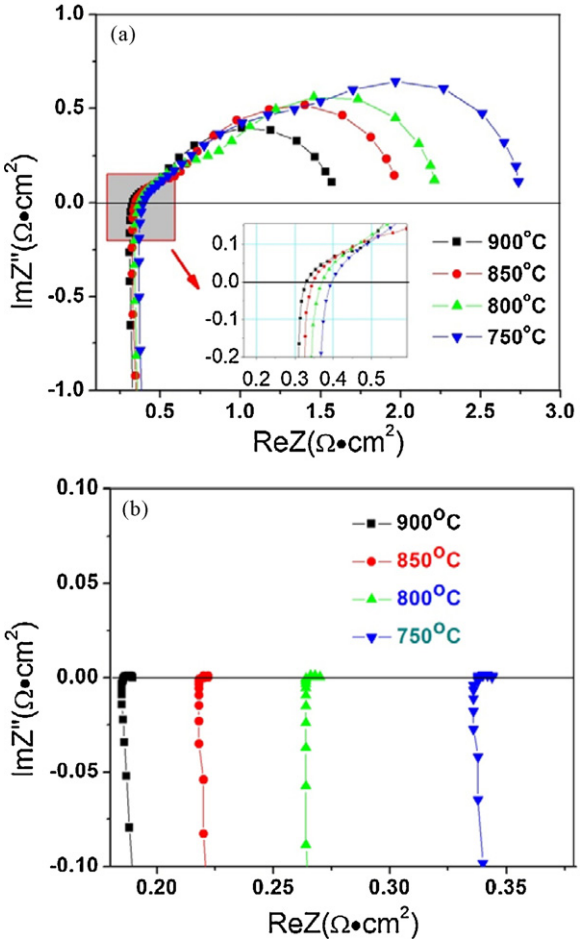

Fig. 3. AC impedance spectra of (a) anode and cathode, (b) anode and interconnector at different temperatures.

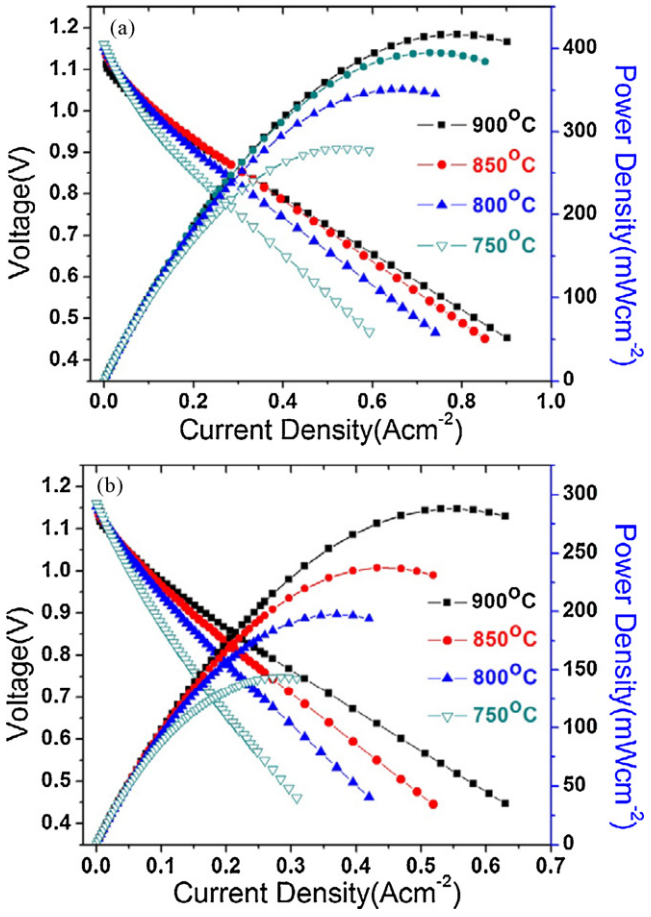

Fig. 4. *I–V* curves and current–power density curves of (a) a cell without interconnector, and (b) a cell with interconnector at different temperatures.

nector, respectively. So the electrochemical impedance spectra (EIS) between anode and interconnector/cathode could be obtained simultaneously. The EIS was measured by an Electrochemical Workstation IM6ex (Zahner, GmbH, Germany), which recorded under open circuit, with an amplitude of 20 mV. The frequency range was 0.03 Hz to 100 kHz for anode–cathode and 0.1 Hz to 100 kHz for anode–interconnector.

To evaluate the impact of interconnector on SOFC power output, current–voltage (*I–V*) curves were employed to compare the performance of single cell with and without interconnector. Humidified hydrogen was used as fuel and oxygen as the oxidant. The fuel and oxidant flow rates were set at 120 mL min^{-1} and 100 mL min^{-1}, respectively. Cells were operated at 900 °C, 850 °C, 800 °C and 750 °C, respectively. Cathode and interconnector area were 8.1 cm^2 and 2 cm^2, respectively.

3. Results and discussion

3.1. Microstructure characteristics of the SLT/LSM interconnector

Fig. 1 shows the SEM micrographs of co-sintered interconnector and anode, with different magnifications. From Fig. 1 we can see the interconnector layer was about 30 μm, and was quite dense despite of few close pores. The interface of SLT layer and LSM layer can barely be seen, which indicated their good combination. The interconnector layer also combined very well with anode. The good combination showed by SEM resulted from the co-sintering method.

Fig. 2 shows the EDS line-scan images through cross-section of co-sintered interconnector and anode. Along the scan direction (A–B) we can see that Mn mainly abounded in the outer layer, from 0 μm to 10 μm; while Ti abounded in the inner layer, from 10 μm to 30 μm. From which we can infer that the thickness of LSM and SLT was about 10 μm and 20 μm, respectively.

3.2. AC impedance spectra between anode and interconnector/cathode

Fig. 3a shows the AC impedance spectra between anode and cathode at different temperatures. The ohmic resistances at 900 °C, 850 °C, 800 °C and 750 °C were about 0.33 Ω cm^2, 0.35 Ω cm^2, 0.37 Ω cm^2, and 0.4 Ω cm^2, respectively, which increased with temperature decreasing. And the polarization resistances followed the same rule with that of ohmic resistances.

Fig. 3b shows the AC impedance spectra between anode and interconnector at different temperatures. The ohmic resistances at 900 °C, 850 °C, 800 °C and 750 °C were about 0.186 Ω cm^2, 0.22 Ω cm^2, 0.265 Ω cm^2, and 0.338 Ω cm^2, respectively, which were smaller than the resistances of anode–cathode at any temperatures. The ohmic resistance significantly reduced at higher temperature, showing that ceramic interconnector possessed more advantages at high temperature.

3.3. I–V curves and power output

Fig. 4 shows the *I–V* curves and current–power density curves of (a) cell without interconnector; (b) cell with interconnector at dif-

Table 1
Maximum power density comparison of cells with and without interconnector at different temperatures.

	900 °C	850 °C	800 °C	750 °C
Cell without interconnector ($mW\,cm^{-2}$)	420	390	350	280
Cell with interconnector ($mW\,cm^{-2}$)	290	240	200	140
Power loss (%)	31	38	43	50

ferent temperatures. From Fig. 4b we can see that OCV at different temperatures were all above 1.1 V, which proved that the interconnector was dense enough. This was consistent with the results of SEM.

The ohmic resistances of cells increased due to the introduction of interconnector, so extra power loss was unavoidable. In order to compare the power output of cells with and without interconnector, maximum power density at different temperatures were listed in Table 1. At 900 °C, The maximum power density was 290 $mW\,cm^{-2}$ for cell with interconnector, and 420 $mW\,cm^{-2}$ for cell without it. There was 30% power loss with this novel bilayered SLT/LSM interconnector, which was acceptable and practicable providing it remains stable in long time. From Table1 we found there was a tendency that the power loss was less at higher temperature, showing that high operating temperature was favorable for ceramic interconnector to reduce power loss.

4. Conclusions

A novel bilayered $Sr_{0.6}La_{0.4}TiO_3/La_{0.8}Sr_{0.2}MnO_3$ interconnector was fabricated by slurry-brushing and co-sintering process, which was a very convenient and cost-effective way to prepare dense interconnector for anode-supported tubular SOFC. SEM micrographs showed that the SLT and LSM layer combined well together. The ohmic resistances between anode and SLT/LSM interconnector at 900 °C, 850 °C, 800 °C and 750 °C were about 0.186 $\Omega\,cm^2$, 0.22 $\Omega\,cm^2$, 0.265 $\Omega\,cm^2$ and 0.338 $\Omega\,cm^2$, respectively, which were smaller than that of anode–cathode at any temperature. At 900 °C, the maximum power density of a cell with interconnector was 290 $mW\,cm^{-2}$, which demonstrated nearly 70% power output compared with the cell without interconnector. Our further work will concern the long-term stability of cells with this bilayered $Sr_{0.6}La_{0.4}TiO_3/La_{0.8}Sr_{0.2}MnO_3$ interconnector.

References

[1] Z. Zhong, Solid State Ionics 177 (2006) 757–764.
[2] W. Huang, S. Gopalan, Solid State Ionics 177 (2006) 347–350.
[3] J.-M. Klein, Y. Bultel, J. Appl. Electrochem. 38 (2008) 497–505.
[4] N. Droushiotis, et al., Electrochem. Commun. 11 (2009) 1799–1802.
[5] N.M. Sammes, Y. Du, R. Bove, J. Power Sources 145 (2005) 428–434.
[6] T. Yamaguchi, et al., Electrochem. Commun. 10 (2008) 1381–1383.
[7] J.W. Fergus, Solid State Ionics 171 (2004) 1–15.
[8] S. Wang, B. Lin, et al., J. Alloy Compd. 479 (2009) 764–768.
[9] S. Ghosh, A.D. Sharma, et al., J. Am. Ceram. Soc. 90 (2007) 3741–3747.
[10] P. Duran, J. Tartaj, J. Eur. Ceram. Soc. 24 (2004) 2619–2629.
[11] K. Hilpert, R.W. Steinbrech, J. Eur. Ceram. Soc. 23 (2003) 3009–3020.
[12] F. Boroomand, E. Wessel, et al., Solid State Ionics 129 (2000) 251–258.
[13] X. Li, H. Zhao, et al., Int. J. Hydrogen Energy 34 (2009) 6407–6414.
[14] Q. Ma, F. Tietz, et al., J. Power Sources 195 (2010) 1920–1925.
[15] M.J. Escudero, J.T.S. Irvine, et al., J. Power Sources 192 (2009) 43–50.
[16] O.A. Marina, et al., Solid State Ionics 149 (2002) 21–28.
[17] R.Z. Liu, S.R. Wang, et al., J. Solid State Electrochem. 13 (2009) 1905–1911.